An Optical Fiber Probe for Planar Waveguides

David N. Green, Zenastra Photonics, August 2001

Introduction and Background

This work involves investigation of the probing of horizontal optical waveguides, planar to the surface of a silicon substrate, for the purpose of Wafer Level Testing (WLT) of devices. The primary technique involves using a custom probe-head, with an array of fibers protruding at an angle, down from the horizontal, as shown in Figure 1a. This geometry was selected such that the body of the probe-head would not contact the surface at initial contact of the fiber tips with the substrate, and with further flexing of the fibers onto the surface, as shown in Figure 1b. This flexing facilitates bringing the fiber tips into angular (pitch) alignment with the horizontal waveguides. The work leverages technology developed for 'passive' alignment during Fiber-to-Wafer Contact (passive FWC) manufacturing processes, especially with regard to alignment grooves inlaid into the wafer surface, and a fiber array 'sandwich' interface, shown in Figure 1c.

The discussions in sections below cover various items found to be of interest during this work, and are organized according to the following headings and subsections:

Basic Fiber Properties *– Geometry; Optics (Numerical Aperture, Bevel Facet, Bending Loss); Flexibility and Strength (Elastic Flexing, Plastic Failure)*

Cantilever Bending Model *– Force and Deflection; Moment, Curvature and Stress*

Practical Probe Design *– Deflection and Clearance (8 mm Fiber Design, 12 mm Fiber Design, 8° Bevel Effect, FWC Trench Crossing); Force and Moment (Probe-Head Force, Vacuum Holding, Sliding Friction); Strain Limits (Bending Stress, Bend Radius)*

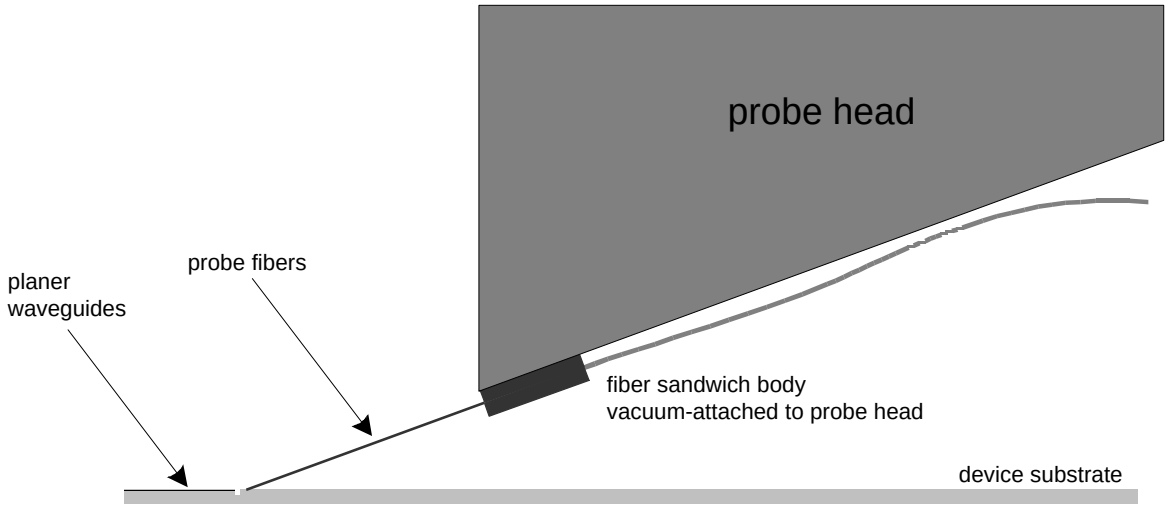

Figure 1a – WLT fiber probe at initial engagement with planar waveguide device.

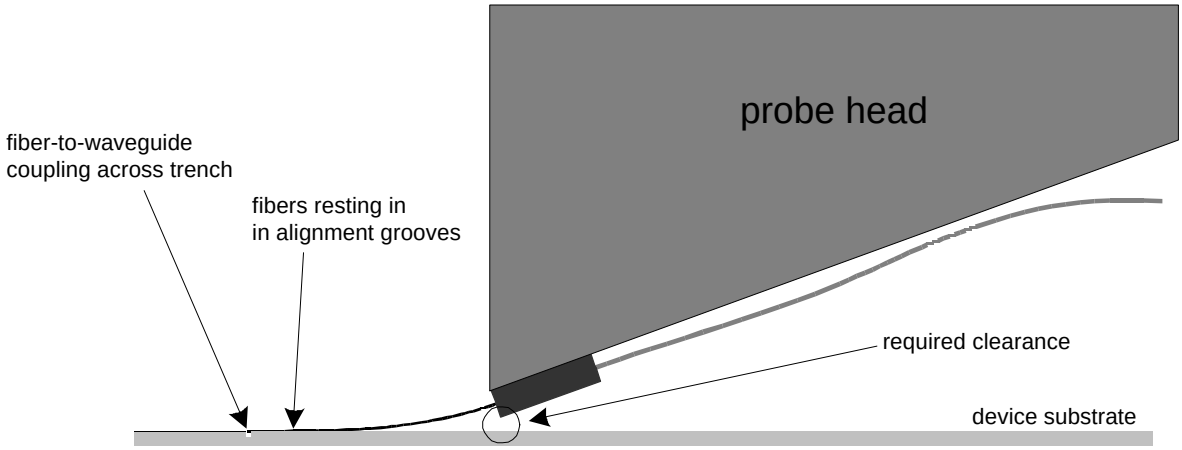

Figure 1b – WLT fiber probe fully engaged with planar waveguide device.

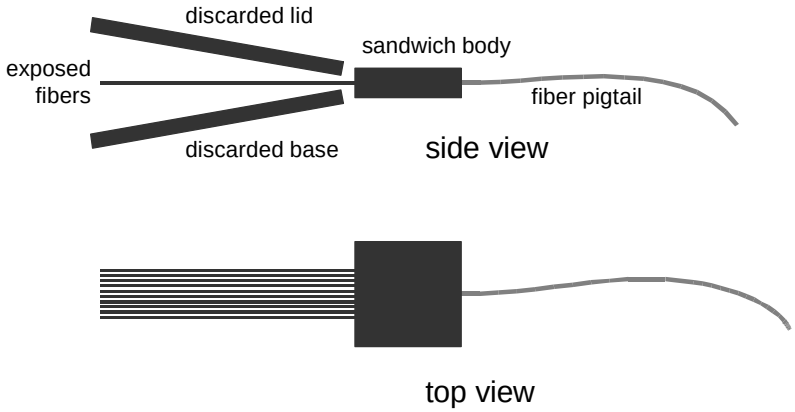

Figure 1c – Passive FWC fiber array sandwich, for use with WLT optical fiber probe.

Basic Fiber Properties

Geometry

The fiber in the WLT probe tip has a circular cross-section, with standard nominal diameter 125 um, and inner core diameter (Corning SMF-28 fiber) of about 8.2 um. (Note the Mode Field Diameter is specified to be about 10.4 um @ 1550 nm wavelength.) This is a cross-sectional area of about 12272 um^2 for the fiber, and 52.8 um^2 for the core. (see Figure 2a) It is noted that the rectangular cross-section planer waveguides, currently in use for this work, have core dimensions of 6 um x 6 um. The fiber tip may also have a beveled (angled) face, with a surface normal that is 8° from the longitudinal axis of the fiber, as shown in Figure 2c.

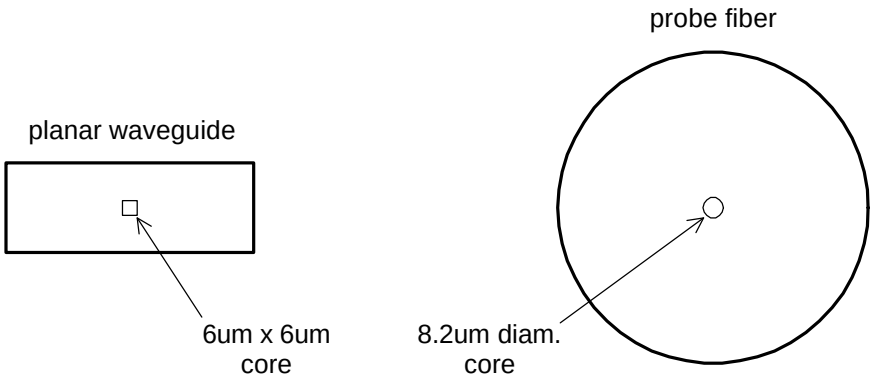

Figure 2a – Cross-section of device waveguide and probe fiber.

Optics

Numerical Aperture

It is assumed that the nominal (effective) index of refraction of the fiber is about $n_{eff} = 1.468$, and the relative core-cladding index difference is $\Delta = 0.0036$ (cladding index 0.36% lower than core; Corning SMF-28 fiber). The numerical aperture of the fiber tip, NA, in open air, is given by

$$NA \approx n_{eff} \sqrt{2\Delta}\,, \qquad (1)$$

such that NA ≈ 0.125. This is equivalent to a maximum entrance angle of $\theta_{NA} \approx 7.16°$, as shown in Figure 2b. (Note: $\theta_{NA} = \sin^{-1} NA$) This angle defines a geometrical limit for light passing through the fiber tip, such that it may propagate within the fiber due to total internal reflection. (Within the fiber, NA ≈ 0.085 or $\theta_{NA} \approx 4.9°$, which is the angle defining the limits for total internal reflection.) Although perhaps theoretically more appropriate for multi-mode (larger diameter) core fiber, numerical aperture is generally handy in characterizing and conveying geometric concepts.

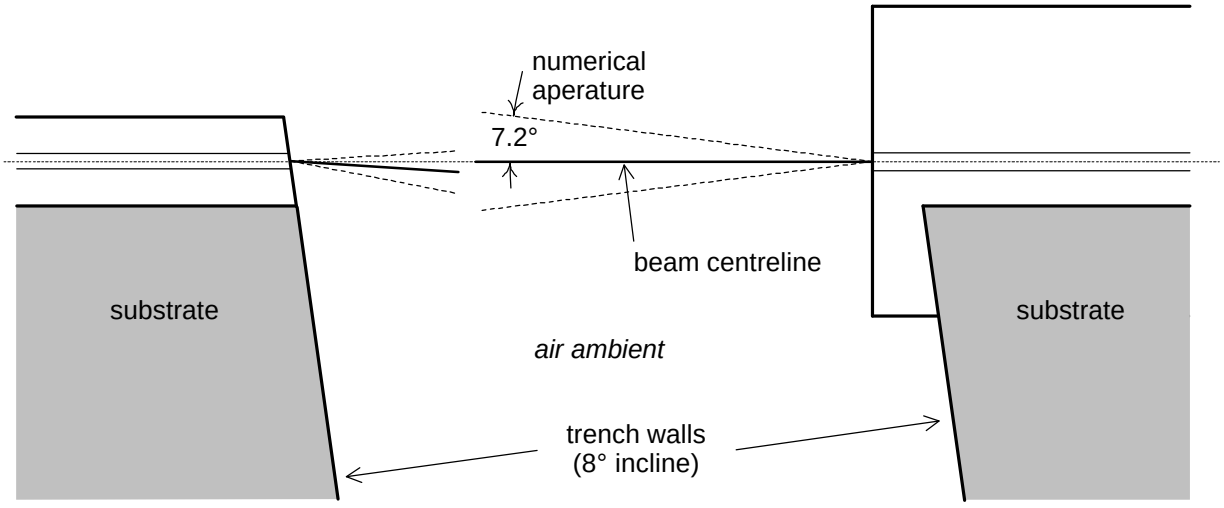

Figure 2b – Basic structure at trench, showing waveguide and fiber apertures.

Bevel Facet

In the case of a bevel at the end of the fiber, the aperture will tilt from the longitudinal axis of the fiber due to refraction. More specifically, the central peak of the amplitude distribution, across the fiber core, will deflect from the longitudinal axis due to refraction at the end face. The amount of deflection at the end face may be found using Snell's Law,

$$n_{air} \sin q_{air} = n_{fbr} \sin q_{fbr}, \qquad (2)$$

where θ_{air} is the angle at which the peak propagates in air, relative to the face normal, θ_{fbr} is the propagation angle in the fiber relative to the face normal, $n_{fbr} \approx n_{eff} \approx 1.468$, and $n_{air} \approx 1$. For a bevel angle of $\theta_{fbr} = 8°$, we find $\theta_{air} \approx 11.8°$, and the total deflection from the longitudinal axis of the fiber is then about 3.8° (11.8° - 8°), as shown in Figure 2c.

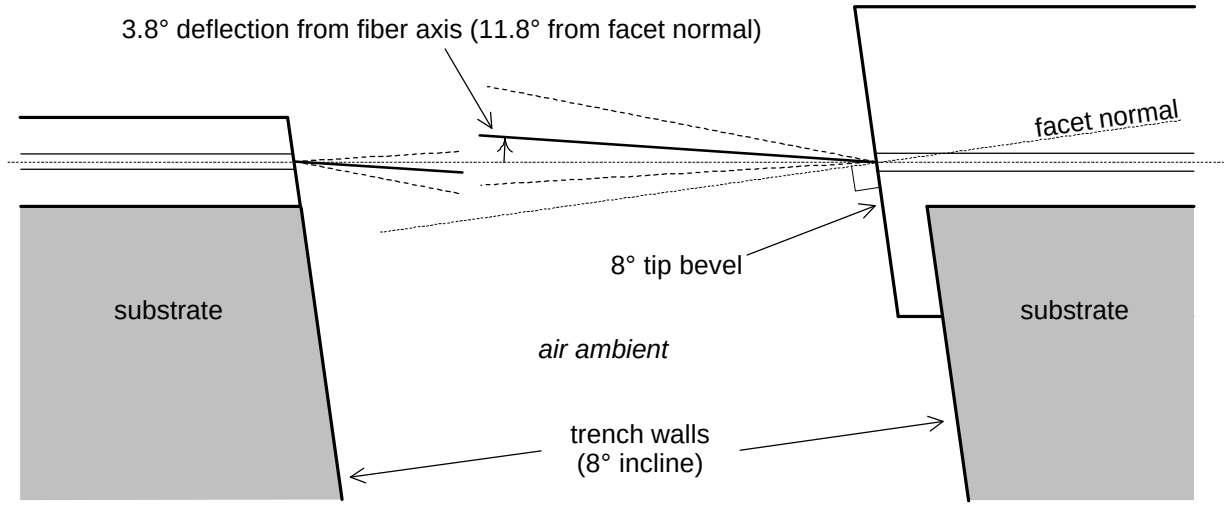

Figure 2c – Deflection of aperture due to refraction at fiber bevel (similar for waveguide).

Bending Loss

A minimum fiber bend radius, below which light will not pass, is essentially a well-defined geometric strain configuration at which total internal reflection cannot be achieved for a given light 'ray', traveling through a given bend in a fiber. For single mode fiber this point seems less well defined, and is maybe better considered as simply a radius below which loss into the cladding is unacceptably high.

For the single mode fiber used in this work, there seems to be a bend radius (ρ) range over which loss is known and reported to become significant. A brief review of various literature suggests this range (for λ=1550nm) is perhaps $\rho \approx 16$ - 25 mm. One applicable specification (Corning SMF-28) indicates about a 0.5 dB loss for one turn (360° bend) around a 32 mm diameter (ρ = 16mm) mandrel. This might be assumed to suggest say about 0.03 dB loss per 22.5° bend; this bend angle is a little greater than the total seen by any fiber in this work. Furthermore, the same specification indicates loss of only about 0.001 dB per turn at bend radius ρ = 25 mm, or say about 0.00006 dB per 22.5° bend. Another published specification (Alcatel), for similar fiber, again at bend radius ρ = 16 mm, simply indicates loss of 0.02 dB per bend.

For the sake of argument in design, we might then specify that any bend radius of $\rho > 25$ mm is surely insignificant, that $\rho \geq 16$ mm would likely be insignificant (a few hundredths of a dB at most), and that $\rho < 16$ mm may be an issue, depending on experimental findings.

Flexibility and Strength

Elastic Flexing

The flexibility of a fiber is a function of it's geometry and it's intrinsic elasticity. The area moment of inertia for a circular section is given by

$$I = \frac{pd^4}{64}, \tag{3}$$

such that for 125 um diameter fiber we have $I \approx 1.2 \times 10^{-5}$ mm^4. Assuming then that modulus of elasticity of the glass is E = 70 GPa, the flexural rigidity of such a fiber is $EI \approx 8.4 \times 10^{-7}$ Nm^2. This quantity characterizes the spring constant for bending the given fiber, the constant itself still being dependent on the fiber length.

Plastic Failure

The plastic deformability of glass under stress (over a short duration) is negligible in comparison to many other materials, such as most metals. Although the stress required for a (rather sudden) fracture may be as high as about 14 GPa, it has been reported that practical fiber fails in a range of say 0.7 - 3.5 GPa, due to stress concentration at randomly distributed flaws in the material. (The specification for Corning SMF-28 fiber indicates that it is tested to at least 0.7 GPa.)

In terms of strain, a brief study of the literature suggests that to avoid mechanical failure, one should avoid continuous flexing (typical on a storage spool) of a fiber at a bend radius less than about 300 times the fiber diameter. In addition, and more likely appropriate for this work, one should avoid momentary flexing (typical of handling during installation) of a fiber to a bend radius of less than about 100 times the fiber diameter. These guidelines suggest that in this work, we might consider a fiber bend radius of say $\rho = 37.5$ mm (=300x125um) to be of no concern mechanically, but that it would be wise to try to keep any bend radius as high above $\rho = 12.5$ mm (=100x125um) as possible.

(It is noted that if one assumes the fiber used here is bent according to the cantilever beam bending model outlined in the discussion to follow, the 37.5 mm and 12.5 mm bending radii correspond to maximum bending stress levels of about 117 MPa and 350 MPa, respectively.)

Cantilever Bending Model

For small lateral deflections of the fiber tip, the mechanics of deformation should be well described by the standard relations for an end-loaded cantilever beam, illustrated in Figure 3.

Force and Deflection

The equation describing the transverse deflection, y, of the end-loaded cantilever beam, shown in Figure 3, is given by

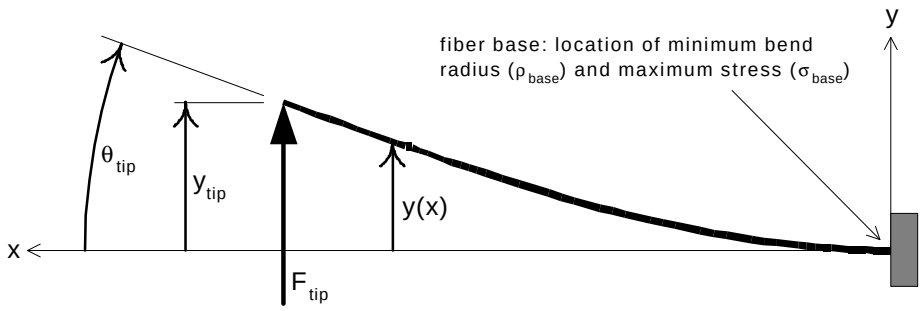

Figure 3 – Fiber bending based on an ideal cantilever beam model.

$$y(x) = \frac{F_{tip}}{6EI}\left(3Lx^2 - x^3\right), \tag{4}$$

where x the distance from the base of the beam, and F_{tip} is the transverse force applied at the end of the beam. The slope along the end-loaded beam may be found by differentiating equation 4, to yield

$$y'(x) = \frac{F_{tip}}{2EI}\left(2Lx - x^2\right). \tag{5}$$

In this work we will be concerned primarily with deflection at the fiber tip. In this case we can set x = L, such that with equation 4, we get the linear tip deflection equation,

$$y_{tip} = \frac{F_{tip}L^3}{3EI}, \tag{6}$$

and from equation 5, the angular tip deflection equation,

$$y'_{tip} = \frac{F_{tip}L^2}{2EI}. \tag{7}$$

Although we will briefly consider forces below, it will be of more interest to consider the direct relationship between angular and linear tip deflection when pressing a fiber onto the wafer surface. Combining equations 6 and 7, and noting that

$$y'_{tip} = \tan q_{tip}, \tag{8}$$

we can find the relationship,

$$\boxed{y_{tip} = \frac{2}{3}L\tan q_{tip}}, \tag{9}$$

where θ_{tip} is the angular deflection of the fiber tip. A plot of this relationship for fibers of 8 mm and 12 mm length is shown in Figure 4. It is noted that force (F_{tip}) and rigidity (EI) do not play a part in the relationship.

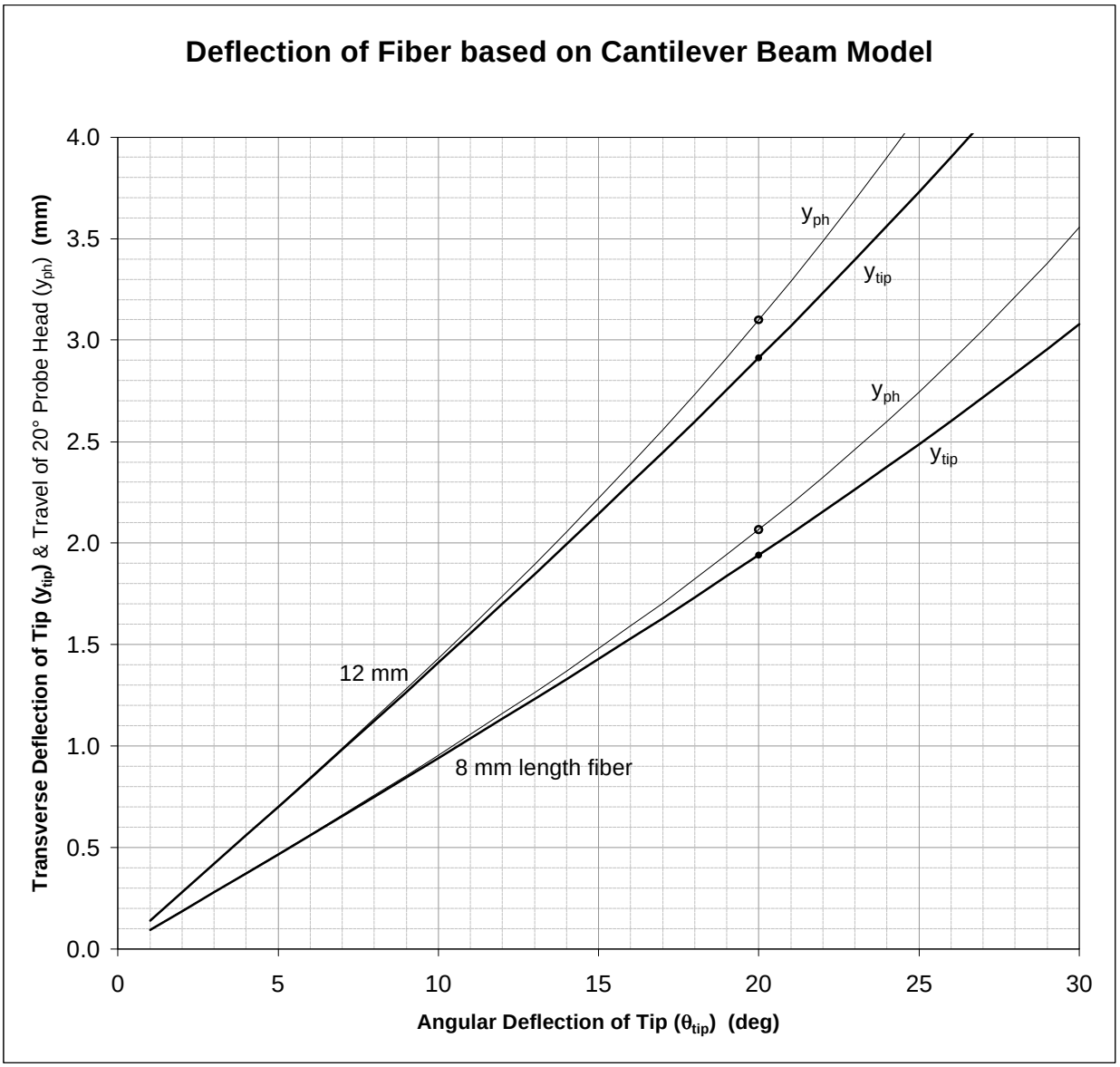

Figure 4 – Theoretical deflection of fiber tip (y_{tip} vs. θ_{tip}), based on cantilever beam model.

Moment, Curvature and Stress

The bending moment, M, at a point along the beam or fiber is given by

$$M(x) = F_{tip}(L - x) \ . \tag{10}$$

The radius of curvature, ρ, of the fiber, due to such a moment, is given by

$$r(x) = \frac{EI}{M(x)} \ , \tag{11}$$

and the compressive and tensile stress, at the inside and outside edges (Fig. 3), respectively, of the curving fiber, is given by

$$s(x) = \frac{M(x)}{I}\left(\frac{d}{2}\right), \tag{12}$$

where d/2 (62.5 um) is the distance from the central (neutral) axis of the fiber to the surface(s).

In this work we will be primarily interested only in the bending at the fiber base (the maximum), such that we can set x = 0 in equation 10. Then substituting this into in equations 11 and 12, in terms of transverse tip force, we have:

$$r_{base} = \frac{EI}{F_{tip}L}, \tag{13}$$

$$s_{base} = \frac{F_{tip}L}{I}\left(\frac{d}{2}\right). \tag{14}$$

Given the familiarity, to many, of the significance of bending radius, it is handy to consider the direct relationship between bending radius and tip deflection when pressing a fiber onto the wafer surface. Using equation 6 or 7, with equation 13, we can solve to find such a relationship. In the case of linear tip deflection, using equations 6 and 13 yields

$$r_{base} = \frac{L^2}{3y_{tip}}. \tag{15}$$

In the case of angular tip deflection, using equations 7 and 13 (with 8) yields

$$r_{base} = \frac{L}{2\tan q_{tip}}. \tag{16}$$

It is noted that force (F_{tip}) and rigidity (EI) do not play a role in these relationships.

Practical Probe Design

The various model relationships, outlined earlier above, were entered into a spreadsheet for iterative exploration of the effect of design parameters. Table 1 contains one state of the spreadsheet. The main parameters adjusted in the design model were the fiber length (L = 8, 10 & 12mm), and the angle at which the sandwich is held by the probe head (θ_{base} = 10, 15, 20 & 25°). The computed results are for a design scenario where the sandwich is held at a fixed angle (θ_{base}), and lowered to a 'depth' (y_{ph}), past initial contact, at which the longitudinal fiber axis, at the tip, is tangent to the wafer surface. (Fig. 5)

It is noted that for most of the scenarios, especially with larger base angles, the cantilever beam model is perhaps being pushed beyond the limits of the small deflection assumptions required for accurate results. It is assumed that the model is still useful for initial design considerations.

The model assumes tip deflection, y_{tip}, is transverse (perpendicular) to the longitudinal axis of the fiber base, as shown in Figure 5. The vertical depth of travel of the fiber base and probe-head, y_{ph}, however, in the current probe-head design, is perpendicular to the contact surface, also as shown in Figure 5. This depth (y_{ph}) is in fact slightly greater in magnitude than that of the transverse deflection of the tip (y_{tip}), in approximately the opposite direction, as defined by

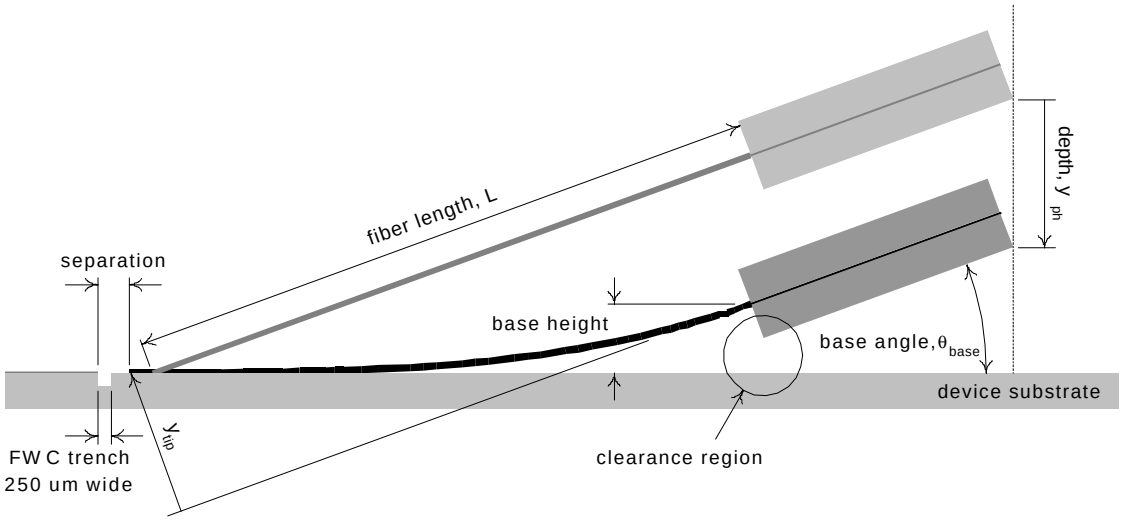

Figure 5 – Significant geometry for fiber probe design.

$$y_{ph} = \frac{y_{tip}}{\cos q_{base}}, \tag{17}$$

where θ_{base} is the angle between the fiber base and the contact surface. The relationship may be observed by comparing the plots of y_{ph} and y_{tip}, each versus θ_{base}, shown in Figure 4. This relationship is also used in Table 1 to compute the probe depth required to achieve the needed tip displacement. Note that the tip angle, θ_{tip} in Equation 9, shown in Figure 3, is assumed to be equal to that required to bring the fiber tip tangent to the contact surface with the current probe head design. It is therefore equal in magnitude to the base angle, θ_{base}, shown in Figure 5, and used in Table 1.

Finally, two particular designs were chosen for further study, and are highlighted in the following subsections. The first uses an 8 mm fiber length and a base angle of 20°, and the second a 12 mm length at the same base angle. The shorter length is standard for the passive FWC work in progress. The longer length seems to comfortably alleviate expected problems with the shorter fiber, while the common base angle reduces mechanical design effort required for development of prototype probe heads.

Deflection and Clearance

The intention of the initial design concept for the probe-head (Fig. 1) was to use the FWC sandwich, already developed, and attach it in such a fashion that the lowest point on the probe would be the fiber tips, with enough clearance to accommodate the body of the sandwich. The height of the fiber base, above the substrate surface, must then always be greater than about half the thickness of the sandwich body (see clearance region in Figure 5). (The half-thickness, about 690 um, is conservative, since at a base angle of say 20°, the lower corner of the sandwich is about 650 um below the fiber base, and this is then in fact the required minimum fiber base

height.) It is noted that the central longitudinal axis of a fiber tip (essentially the core) sits very near the upper-most surface of the substrate when the fiber is in the alignment groove.

8 mm Fiber Design

From Table 1 we can see that for an 8 mm fiber sandwich, a 20° base angle would require about 2066 um depth of travel of the probe head (y_{tip} = 1941um, y_{ph} = 2066um), beyond initial contact of the fiber tips with the substrate surface. This would result in about 670 um base height, which appears to be about the maximum possible using an 8 mm fiber. (15° and 25° base angles yield less) This is too close to ensure clearance between the sandwich body and wafer substrate, however in the case of singulated devices, only the fiber tips need be over (contacting) the device, and the sandwich body can be located beyond the edge of the device. This situation offers an extra clearance of about 670 um (device substrate thickness).

12 mm Fiber Design

Using the same basic probe-head design, the fibers may be lengthened to increase the final height of the fiber base, both at initial tip contact, and when the pressed to bring the tips tangent to the surface. The spreadsheet results in Table 1 indicate that a 12 mm fiber sandwich, still at a 20° base angle, would require about 3099 um depth of travel of the probe head, for tangential contact. This would still leave about 1006 um fiber base height, which should be sufficient to accommodate the lower half of the sandwich body.

8° Bevel Effect

For the 8° beveled tip fiber, discussed in an earlier section, the longitudinal axis of the fiber tip is required only to come within about 3.8° of reaching tangency with the contact surface, at which point the 'upward' refracting central axis of the aperture will already be parallel to the wafer, as illustrated in Figure 6. This means that, for example, with a base angle of θ_{base} = 20°, the fiber tip angle (Fig. 3) needs only to reach $\theta_{tip} \approx 16.2°$. Using the above relationships (equations 9 and 17) it is found that for the 8 mm fiber, at base angle 20°, the required probe travel depth is only y_{ph} = 1650 um (y_{tip} = 1550um), compared to 2066 um computed above for fiber with no bevel at the tip. Similarly, for 12 mm length fiber with a beveled tip, we require only y_{ph} = 2475 um to bring the aperture central axis parallel to the surface, compared to 3099 um for no bevel.

There is a possibility of increased difficulty in controlling tip (pitch) angle with the beveled-tip application considered above, in comparison to the application where the fiber tip may brought to fully tangent contact. Also, there may be increased tendency for the lower edge of the fiber tip to catch irregularities in the contact surface during longitudinal (separation) motion.

It is noted that if an index matching fluid is applied between each fiber tip and device waveguide facet, such as it is during normal FWC bonding, refraction may be significantly reduced, such that the aperture of the beveled fiber (and of the mating waveguide) tends to return to alignment with the longitudinal axis of the fiber core. A similar matching of indices might allow beveled fiber to be used in the 'normal' probe application described above earlier, where the probe head is driven down to the point where the tip is again fully tangent to the contact surface. However, given that reducing back-reflection (using a beveled tip facet) is not of critical importance in the practical WLT measurement scenario, it is likely better to maximize potential signal transmission, and reduce positional sensitivities, by using tangential tip contact, with no bevel.

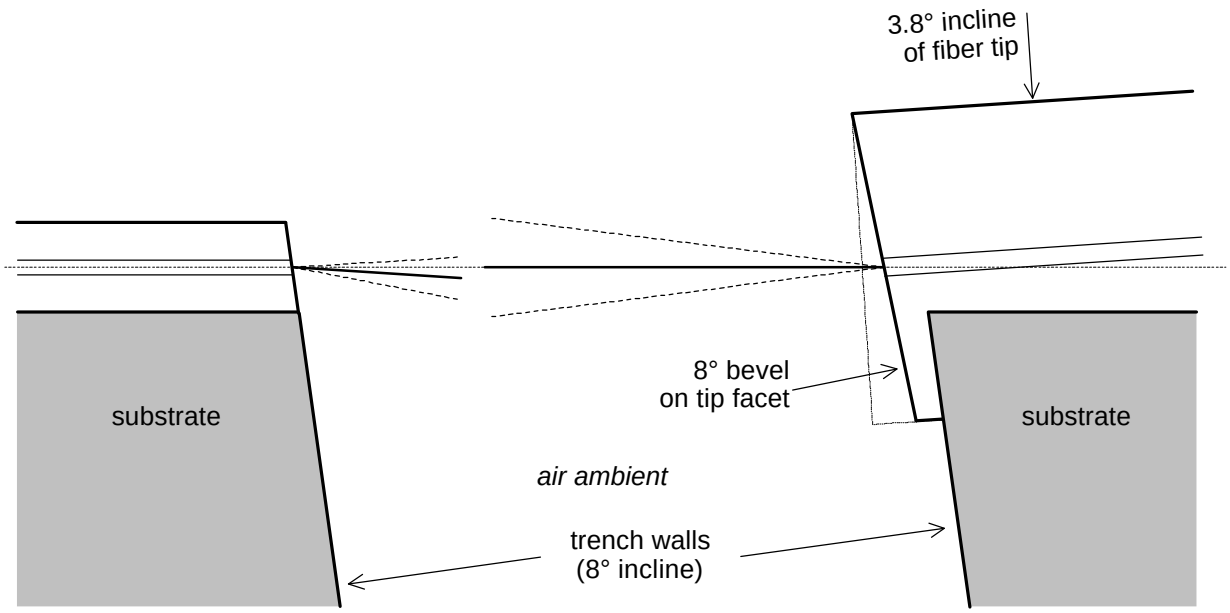

Figure 6 – Incline of beveled fiber tip, to lower upward-refracted aperture down to horizontal.

FWC Trench Crossing

To facilitate extension of the probe tip over a trench, we should account for the fact that the fiber contact point cannot be at the tip of the fiber, as may be seen in Figure 7a. Assuming that the 'free' fiber end is relatively straight, then this extended portion of fiber will be axially aligned with the fiber which is in contact with the groove surface. To (pitch) align the fiber tip, we must then bring the contact point, at the end of the now shorter flexing fiber section, tangent to the substrate.

In the extreme application, involving near contact between fiber tip and waveguide facet, the modeled fiber length must be reduced by the full width of the FWC trench, or typically as much as 250 um. This results in model lengths of 7.75 mm and 11.75 mm, for the 8 mm and 12 mm designs, respectively. Using equations 9 and 17, we compute the required depth of travel, y_{ph}, to be about 2001 um and 3034 um, for the 8 mm and 12 mm fiber designs, respectively. The shorter bending sections require less probe depth of travel than do the full length fiber applications noted in Table 1 (where the depths are 2066um & 3099um).

The practical (and modeled) application, however, uses a zero-depth reference (initial contact with the surface) taken using the full length of the fiber. In both designs highlighted in this work, 8 mm and 12 mm, the base angle is set to 20°. The 'extra' 250 um of fiber, at the tips, then requires an additional depth of travel of about 86 um (250um x sin 20°) in each case, as may be seen in Figure 7b. This results in a total required depth of travel, y_{ph}, of 2087 um (86+2001) for the 8 mm design, and 3120 um (86+3034) for the 12 mm design. These may be compared to the slightly lower values of 2066 um and 3099 um in Table 1, respectively, for application where contact is expected to be made at only the very tip of the fiber.

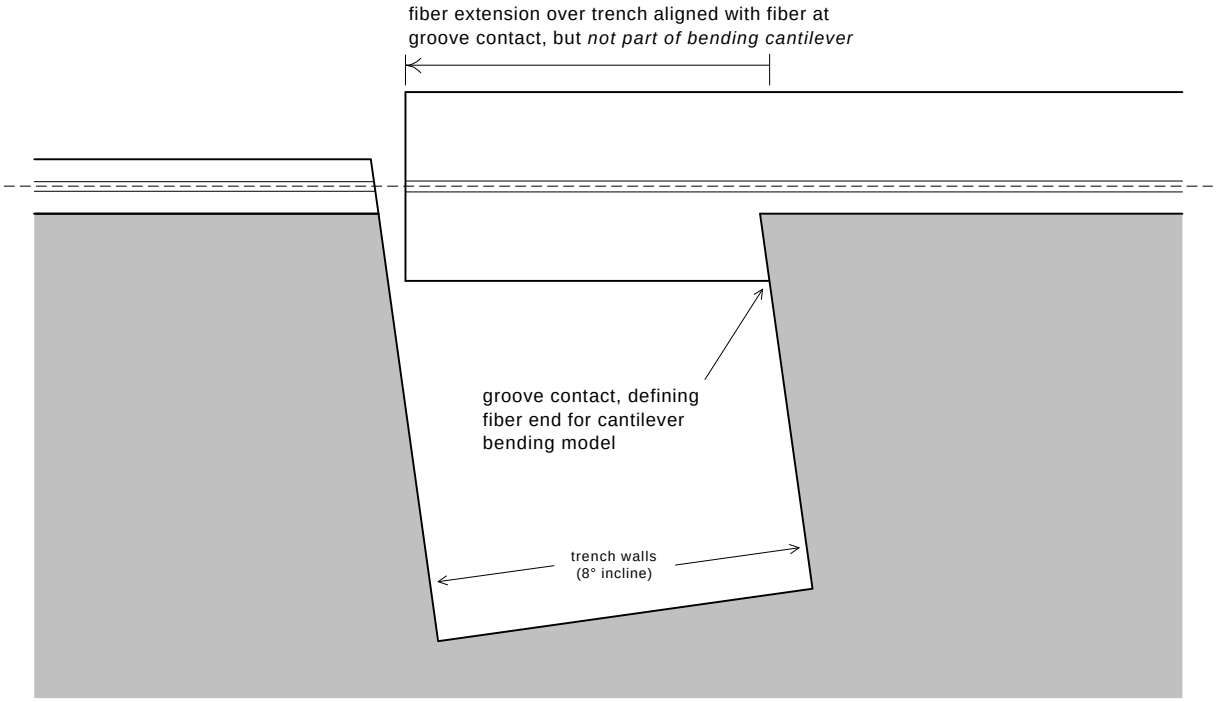

Figure 7a – Extension of fiber tip over trench.

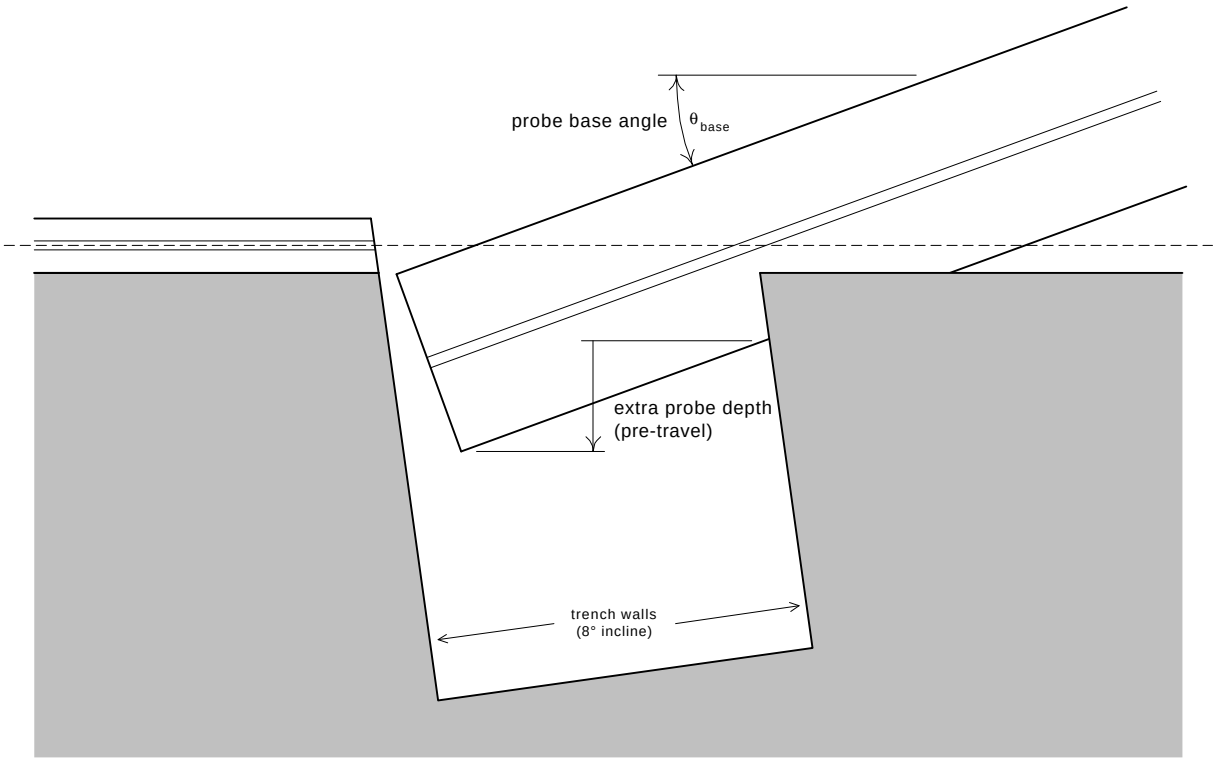

Figure 7b – Extra depth of travel required to make groove contact farther back on fiber.

Force and Moment

The contact force near the fiber tip, and the resulting bending moment at the base, where it is at a maximum, are important parameters with regard to holding and manipulating the probe. (Effects of the accompanying stress and strain are discussed in the next section.) The transverse tip force and base bending moment increase for probe designs with greater base angle, but decrease with increasing fiber length, as may be observed in Table 1. For the 8 mm (at 20°) probe design, we have a tip force of about 9.54 x 10^{-3} N, and maximum bending moment of about 76.3 x 10^{-6} Nm; for the 12 mm design, 4.24 x 10^{-3} N and 50.9 x 10^{-6} Nm.

Probe-Head Force

In practical application, it is expected that the probe head might use a fiber sandwich with an array of perhaps 10 fibers, increasing the required probe force proportionally. In addition, it is noted that the downward force of the probe head is not quite parallel to the opposing transverse force at the fiber tip, as illustrated in Figure 8. Similar to Equation 16 (for probe-head displacement as a function of tip displacement), the vertical probe-head force, F_{ph}, is given by,

$$F_{ph} = \frac{F_{tip}}{\cos q_{base}}, \tag{18}$$

where F_{tip} is the force at the fiber tip, transverse to the fiber at its base, and θ_{base} is the angle of the base or sandwich body. Applying this equation to the single fiber forces noted above, and then increasing them by a factor of 10 to account for a 10-fiber array, we have a total vertical probe-head force of about 0.102 N for the 8 mm design (θ_{base} = 20°), and 0.045 N for the 12 mm design.

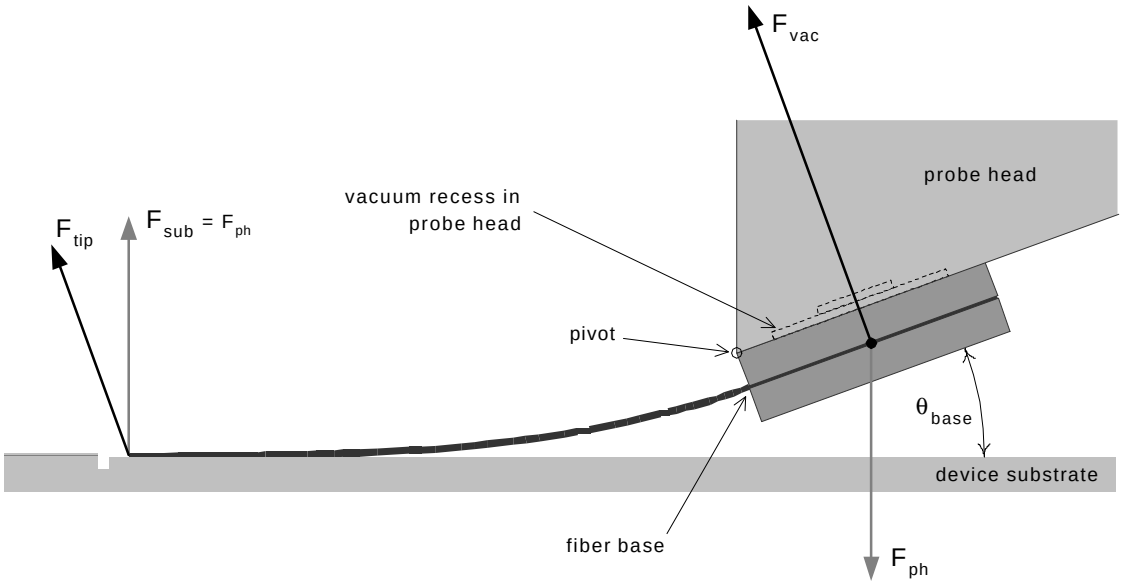

Figure 8 – Vacuum (F_{vac}) countering computed tip force (F_{tip}), about pivot on sandwich body.

Vacuum Holding

The ability to fix the fiber array sandwich body to the probe head may also be of concern. The current design approach is to use vacuum to hold the upper lid of the sandwich body to the bottom of the probe head, as may be observed in Figure 8. Assuming the sandwich is restrained from sliding on the surface, the primary function of the vacuum is to counter the moment at the upper front edge of the sandwich body, where it will pivot during probing, if the vacuum cannot hold. Given that this pivot point is located very close to the fiber base, the counter moment, required to hold the sandwich from pulling away, will be approximately equal to the maximum bending moment at the base of the fibers. The total moment required for a 10-fiber sandwich, based on the single fiber values noted above, is then about 763 x 10^{-6} Nm for the 8mm/20° design, and 509 x 10^{-6} Nm for the 12mm/20° design.

A current design utilizes a vacuum hole (square recess in the probe-head surface) of about 10 mm^2 area, centred about 2 mm back from the forward edge (pivot for upset) of the sandwich body, as shown in Figure 8. Assuming a vacuum-side pressure as low as say 1/3 atmosphere, or about 34 kPa (≈4.9psi), we have a pressure differential of 2/3 atmosphere, or about 68 kPa, pushing the sandwich onto the underside of the probe head. For the above vacuum hole, this is then a force of about 0.68 N (68kPa x 10mm^2), and moment, about the noted pivot, of about 1360 x 10^{-6} Nm (0.68N x 2mm). This seems to be about twice the holding moment required for the highlighted probe-head designs (763x10^{-6} & 509x10^{-6} Nm) when securing a 10-fiber array.

Sliding Friction

With regard to longitudinal fiber position for waveguide-to-fiber 'separation' (see Fig. 5), it is believed that static friction effects, or 'stiction', may be significant. This phenomenon results from a significant difference between static and dynamic friction forces, acting along the contact between the fiber and groove surfaces. The higher force required to get the surfaces to ‘break free’ will add potential energy (elastically) into the fiber prior to sliding, such that the there will be significant 'jumping' prior to relatively smooth sliding.

The glass fiber is very stiff along its longitudinal axis, and will not likely show much stiction effect if driven closely along that axis. However, the higher compliance (in columnar buckling) of the highly bent fiber (20°) could increase the stiction effect, increasing both longitudinal separation error and (perhaps more substantially) angular (pitch) error at the tip. This effect was not investigated for this work. However, ad hoc visual observation in experimental trials indicates that buckling does occur, although it is not clear if it is a significant factor.

Strain Limits

Bending Stress

The maximum stress, due to bending, will occur at the inner and outer bend surface at the base of the cantilevered fiber, as indicated in Figure 3. The compression, at the inner bend surface, and tension, at the outer surface, are theoretically equal in magnitude. Other compressive and shear stresses are expected to be of much less concern, and are not considered in this discussion.

Increasing the base angle (θ_{base}) increases the maximum stress, while lengthening the fiber decreases stress, as may be observed in the data shown in Table 1. The maximum stress is shown to be about 398 MPa and 265 MPa, for each of the 8mm/20° and 12mm/20° designs,

respectively. This seems to be relatively close to the lower value of the failure range, noted earlier to be 700 MPa. Therefore it is speculated that with the highlighted designs, one should probably expect at lest occasional fiber failure due to bending stress, in normal use.

Bend Radius

As a complement to considering maximum stress, one may consider bending limits in terms of the associated strain. Minimum bend radius is very commonly used to specify strain limits for fiber handling and use. Table 1 lists the smallest (tightest) bend radius, at the fiber base, computed for each design, where it may be observed that this radius decreases for increasing base angle, and increases with increasing fiber length. The base bend radius for the 8mm/20° and 12mm/20° designs is found to be ρ = 11.0 mm and ρ = 16.5 mm, respectively.

The minimum range over which one might begin to encounter mechanical (failure) problems was suggested in an earlier section to begin at about ρ = 37.5 mm, and reach perhaps a 'critical' level somewhere near say ρ = 12.5 mm. According to these guidelines, one might expect to encounter some notable amount fiber breakage with use of either probe design, particularly for 8 mm fiber.

The radius under which one might begin to encounter measurably significant power loss (say more than a few hundredths of a dB) was suggested earlier to be approximately ρ = 16 mm. According to this guideline, one might expect some measurable, if not significant, level of loss with the 12 mm design (ρ=16.5mm), and perhaps significant loss with the 8 mm design (ρ=11.0mm). It is noted that early experiments have shown that there seems to be little significant loss for the 12mm design, and that loss is in no way crippling for either design.

Fiber Probe Cantilever Model

elastic modulus E (GPa) :	70						
fiber diameter (um) :	125						
area moment of inertia I (mm^4) :	1.20 E-5						
flexural rigidity EI (Nm^2) :	8.39 E-7						
fiber length (mm) :	8	8	**8**	8	10	**12**
fiber base angle, θ_{base} (deg) :	10	15	**20**	25	20	**20**
transverse fiber tip force ($N \times 10^{-3}$) :	4.62	7.02	9.54	12.22	6.11	4.24
bending moment at fiber base ($Nm \times 10^{-6}$) :	37.0	56.2	76.3	97.8	61.1	50.9
maximum stress at fiber base (MPa) :	193	293	**398**	510	318	**265**
radius of curvature at fiber base (mm) :	22.7	14.9	**11.0**	8.6	13.7	**16.5**
height of fiber base at initial tip contact (um) :	1389	2071	2736	3381	3420	4104
transverse displacement of fiber tip, y_{tip} (um) :	940	1429	1941	2487	2426	2912
depth of travel of probe head, y_{ph} (um) :	955	1479	**2066**	2744	2582	**3099**
height of fiber base after bending (um) :	434	591	**670**	637	838	**1006**

Table 1 – Fiber probe parameters for various fiber lengths, and initial contact (or base) angles.

Summary of Fiber Probe Parameters

fiber diameter	125 um (area = 12272 um^2)
core diameter	8.2 um (area = 52.8 um^2)
n_{eff} nominal refractive index of fiber	1.468
Δ core-cladding index difference	0.0036 (0.36%)
NA fiber tip aperture	0.125
θ_{NA} maximum entrance angle	7.16°
θ_{TIR} critical angle, internal reflection	4.9°
refractive deflection due to 8° bevel in air	3.79°
EI flexural rigidity of fiber (bending)	8.4 x 10^{-7} Nm^2
I area moment of inertia	1.2 x 10^{-5} mm^4
σ_{me} stress required for fracture	700 MPa - 3500 MPa (14 GPa ultimate)
y_{ph} travel depth for 12mm/20° probe design	3099 um (1006 um fiber base height)
8mm/20° probe	2066 um (670 um fiber base height)
vertical force, 10-fiber array, 12mm/20° probe	0.045 N (4.6 g)
8mm/20° probe	0.102 N (10.4 g)
ρ_{base} base radius of curvature for 12mm/20° probe	16.5 mm
8mm/20° probe	11.0 mm
ρ_{op} minimum radius to avoid significant loss	16 mm (0.02 - 0.04 dB loss spec)
ρ_{me} minimum radius to avoid breakage	12.5 mm (ideally > 37.5 mm)